Hybrid Finite Element-Geometric Forming Simulation Of Composite Materials

Mehran Ebrahimi, Matt Thorn

Autodesk Inc.

ABSTRACT

Computer simulations can extensively help engineers to gain a better understanding of the fabrication processes prior to actually applying them, thus avoiding the manufacturing costs associated with trial-and-error for creating new designs. Of particular importance is fiber-reinforced composite material parts, as their fabrication cost is comparably higher than traditional materials such as metals. In this paper, a hybrid finite element-geometric algorithm for draping simulation of woven fabric composites over a triangulated 3D surface is described. In this algorithm, the composite fabric is characterized as a group of square or rectangular cells modeled via six springs to which a set of physical equations is applied. The values of spring constants are representative of the actual material properties. Hence, compared to purely geometrical methods, this algorithm leads to a more accurate simulation of wrinkles and distortions, and converges significantly faster than purely finite element approaches. The flat contour can also be produced naturally along with the draping simulation.

1. INTRODUCTION

Nowadays, in the era of automation and advanced manufacturing techniques, computer simulations imitating real physical phenomena could help engineers to avoid the time-consuming process of trial-and-error for creating new designs. Consequently, developing more reliable computer-aided-design (CAD) tools is a necessity in today's boom of new fabrication technologies. By connecting design and simulation, engineers can make decisions about downstream behavior like structural performance and manufacturing properties prior to making costly mistakes. This workflow is most optimal when a user can quickly understand physical process and incorporate them back into the design as soon as possible. However, typical finite element solutions take large amounts of time and compute power to get a good result. What if the accuracy of a finite element solution could be combined with an explicit geometric approach to solve for a solution more quickly?

In this paper, a hybrid finite element-geometric algorithm for draping simulation of woven fabric composites over a triangulated 3D surface is described and shown how this approach can also apply to the forming process. Unlike standard kinematic approaches [1], [2], this method incorporates geometry as well as material properties in the solution. The structural properties representing actual mechanical properties of composite materials are considered without affecting the speed of the solution. This technique is built upon the fact that the fabric layers are optimal when the amount of distortions (wrinkles) are at a minimum. This assumption causes the calculation to be extremely fast with minimal forfeit of accuracy when compared to a true finite

element solution. The forming process is becoming more popular in the automotive and construction industries as process constraints and cycle times are driving change in traditional manufacturing processes. Although the target industries here are those designing and manufacturing composite parts, this technique can be leveraged in all fabric-related industries.

In this algorithm, a fabric, before draping, is considered as a group of square (or rectangular) cells, and each cell is modeled by four side-springs and two diagonal springs (Figure 1). These assumptions cause a trade-off between accuracy and speed of draping simulation. However, the generated results could be trustworthy for the majority of cases, and if more accurate modeling is required, other techniques exploiting pure finite element analysis (FEA) [3]–[7] could be implemented with considerably higher computational costs (seconds vs hours).

After draping, a fabric is balanced and consequently has the minimum number of wrinkles (minimum distortion energy) when the resultant force of all springs connected to a node is zero. Therefore, to ensure this condition, at each iteration of the algorithm, to map new cells onto the 3D surface, force balance equations of the engaged nodes are solved. More details will be provided in the following sections.

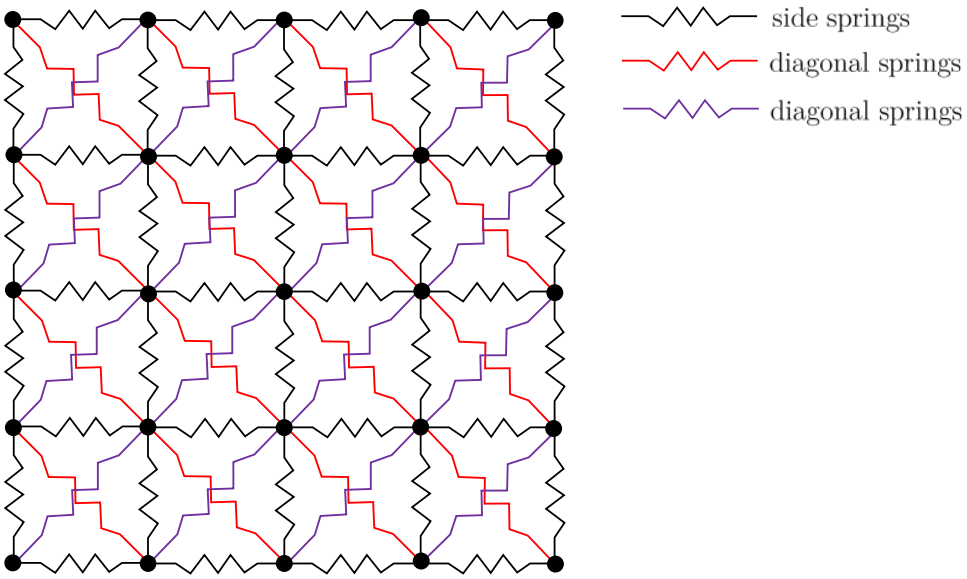

Figure 1- Fabric cells represented by six springs

In the draping process, depending on the surface geometry, the fabric can wrinkle and cells may distort and no longer be a perfect square (or rectangle). Shear angle, defined by Equation 1, at each fabric node is used as a representation of wrinkles in the fabric at that location (Figure 2). In other words, the higher the shear angle is, the more severe the wrinkles are at that location.

$$Shear\ Angle\ \gamma = \frac{\pi}{2} - \alpha. \tag{1}$$

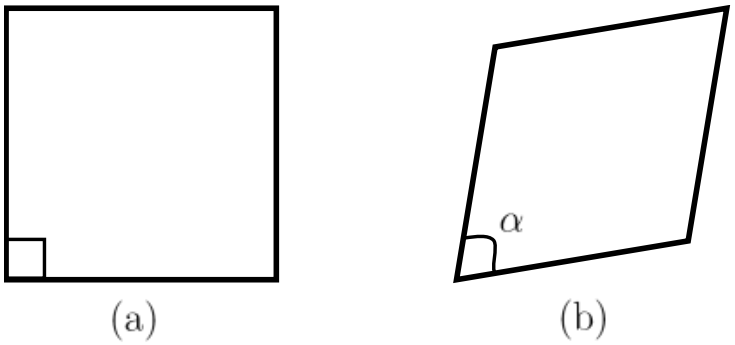

Figure 2- (a) undistorted cell (b) distorted cell

At each fabric node, the shear angle is the weighted average of the shear angles around that node.

2. DRAPING ALGORITHM

Unlike FEA-based methods that require an initial flat (2D) fabric as an input, the algorithm described in this paper does not initiate the simulation from a 2D pattern. This is another advantage of this method over these techniques.

There are two ways of initiating the draping algorithm:

1- From a given starting point P_0 (seed point) and propagation direction t_0 (local fiber orientation at the seed point)
2- From a given starting point P_0 (seed point) and a guide curve c_0.

The difference between the two methods will be explained in the following sections. Other required inputs are:

- S: the triangulated surface to be covered by the fabric
- L_{warp}, L_{weft}: fabric cell size along the sides
- $k_{side}/k_{diagonal}$: the ratio of spring constants along the sides and diagonal directions. The higher this value, the more resistant the fabric is against stretching along the sides versus that along diagonals, which results in shear. For isotropic fabrics (which behave like unidirectional fabrics), this parameter is close to 1. For fabric composites, it typically has a large value, around 200.
- b: surface boundary, the boundary of the area of surface S to be covered by the fabric
- d: Dart curve, if there is any

The values of spring constants can be achieved through well-known physical experiments such as uniaxial tension or picture frame tests. The algorithm, then, proceeds in the following principal steps:

2.1 Perpendicular geodesic paths

Geodesic calculations are required to propagate fabric cells on surface S. A geodesic path on a surface is the shortest path between different points on that surface. In this step, two perpendicular

geodesic paths, along t_0 (warp direction) and perpendicular to t_0 (t_1) (weft direction), are computed passing through P_0 to the surface boundaries. The algorithm used for geodesic calculations can be found in [8]. The very same computation is also performed along $-t_0$ and $-t_1$. Then, these geodesic paths need to be discretized into a number of equidistance nodes according to L_{warp} and L_{weft}. The nodes produced, called anchor nodes, are the first fabric nodes on the surface (Figure 3) whose positions remain fixed throughout the fitting process.

If instead of t_0, a guide curve, c_0, is provided, first this curve is discretized according to L_{warp} and L_{weft} and also a geodesic path perpendicular to c_0 starting from P_0 is computed and discretized. The rest of the process is the same as in the first case.

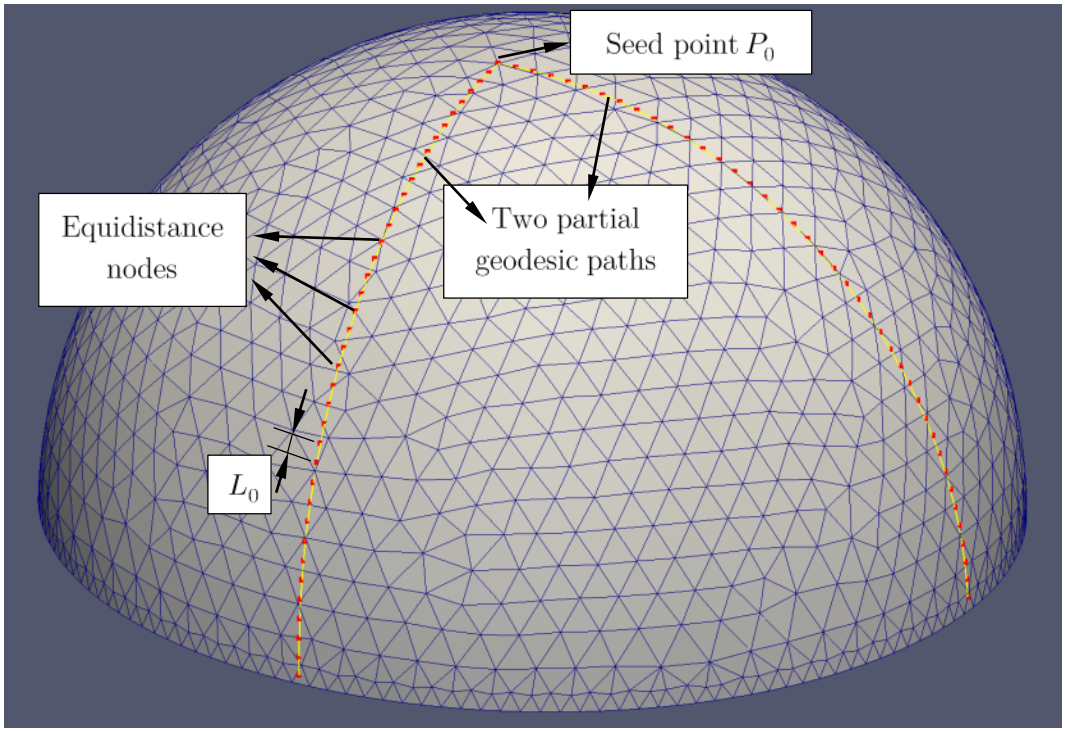

Figure 3- Discretized geodesic paths on a hemisphere

At the end of this step, the surface is split into 4 quadrants (Figure 4). All the remaining computations, in the rest of the draping algorithm, could be performed independently, and so in parallel, in each of these quadrants. This powerful feature reduces the computation time considerably as compared to other techniques available in other commercial products.

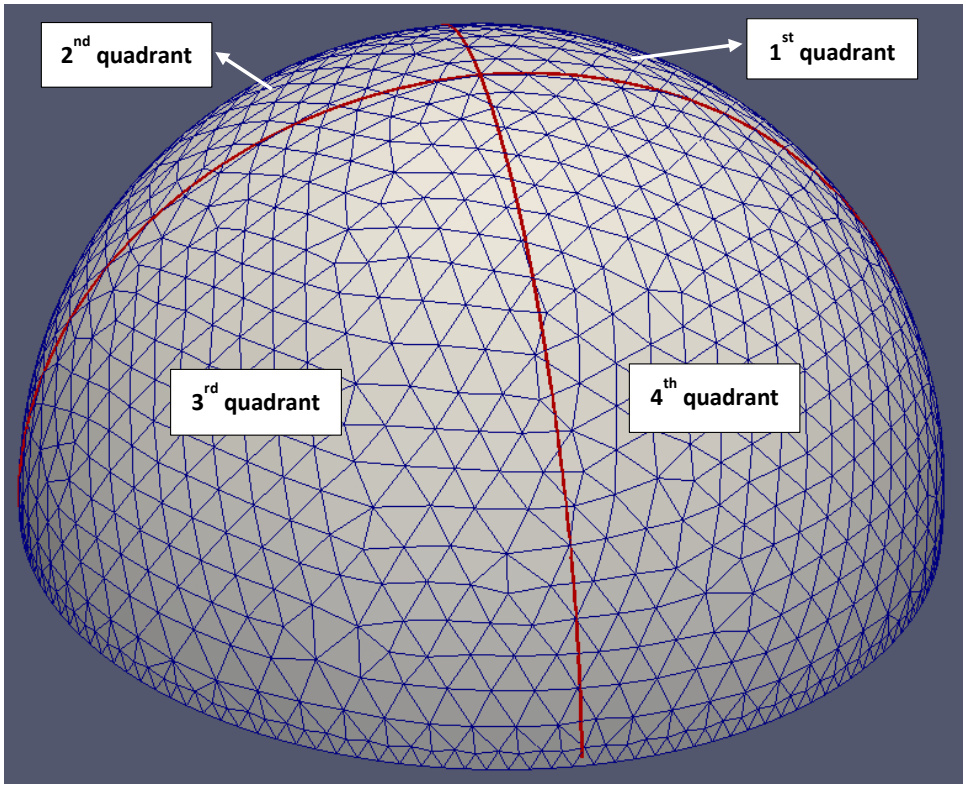

Figure 4- Splitting the surface into four quadrants

2.2 Cell propagation

A cell can be propagated if the position of its three nodes is known and only the location of one node is unknown. Since after the draping process, no external force is exerted on the fabric, total internal forces of each node from the springs linked to it should also be zero.

2.2.1 Partial cell propagation

To locate the fourth node of a cell, Equation 2 should be solved.

$$\sum_{i=1}^{N}(F_i)_{internal} = \sum_{i=1}^{N} k_i \Delta l_i \frac{\vec{X}_i - \vec{X}_{node\ 4}}{\left\|\vec{X}_i - \vec{X}_{node\ 4}\right\|_2} = 0, \qquad (2)$$

$$\Delta l_i = l_i - (L_0)_i, \qquad (a,b)$$

where N is the number of springs connected to this node, $\vec{X}_{node\ 4}$ is the position of the fourth node on the surface (unknown) and $\vec{X}_i$ is the position of adjacent fabric nodes to the fourth nodes (node 4). The important point here is that l_i is not a Euclidean length. In fact, it is the length of the geodesic path connecting the fourth node to other surrounding nodes. Thus, Equation 2 may not have an exact one-step solution for $\vec{X}_{node\ 4}$ and should be solved iteratively. Stopping criterion could be $\sum_{i=1}^{N} F_i < \varepsilon$ (e.g. 10^{-6}) This process is repeated to generate all possible cells. This step of cell propagation is called partial cell propagation.

In this step, also, some parallelization could be done. Once a new cell is propagated on the surface (Figure 5 a), possible cells along the warp and weft directions could be mapped independently and in parallel on the surface (Figure 5 b).

2.2.2 Complete cell propagation

For some geometries, however, partial cell propagation, by the procedure explained, could leave some areas uncovered. In these cases, there are no more three adjacent free nodes left to locate the fourth node of a cell. If this happens, the nodes on the outer boundary of the fabric should be detected, and for one of them, another node is located along the warp or weft directions. Then, it is checked to see by this extension whether new cells can be generated or not. If so, new cells are propagated, otherwise, the same procedure is applied to another node. This process continues until the entire area is covered or the surface boundary is detected. This step of cell propagation is called complete cell propagation. A simplified overview of cell propagation step is described in Figure 5.

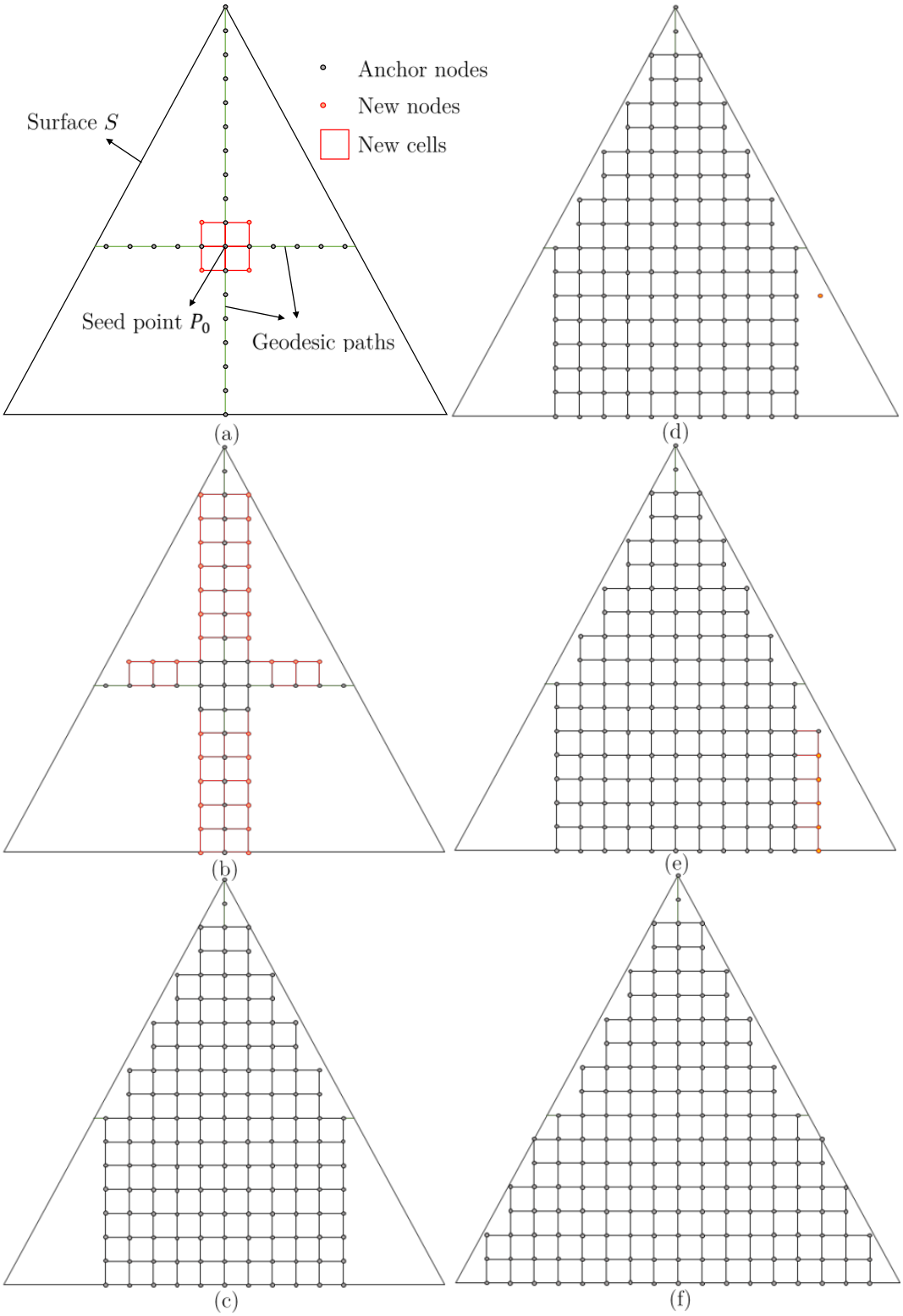

Figure 5- Cell propagation step: (a) generating anchor nodes and first cells (b) Propagating next layer of cells (c) Completing partial cell propagation (d) Placing a node along warp/weft (e) Propagating new cells (f) Cell propagation step completed

2.3 Global balance of nodal internal forces

Although Equation 2 is locally solved for all nodes, by propagating new nodes this constraint could be violated for some nodes. Thus, after the cell propagation step, for all nodes, Equation 2 is checked, and if required their position is changed until total internal spring forces at each node is within the predefined tolerance.

Figure 6, 7 and 8 show draping results of fabric composite for a number of geometries.

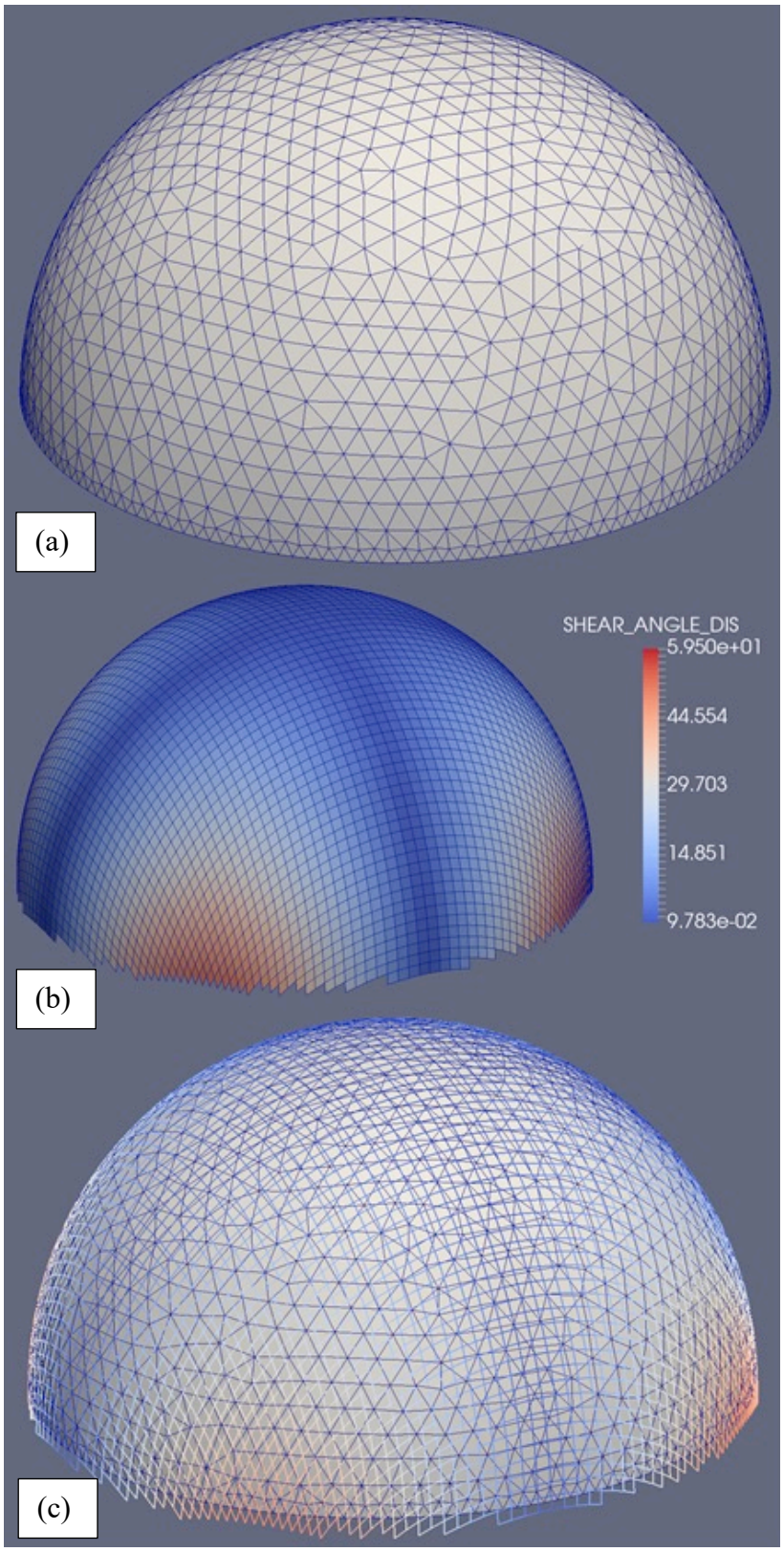

Figure 6- (a) A triangulated hemisphere (b) Shear angle distribution of the draped composite (c) The hemisphere and draped composite together

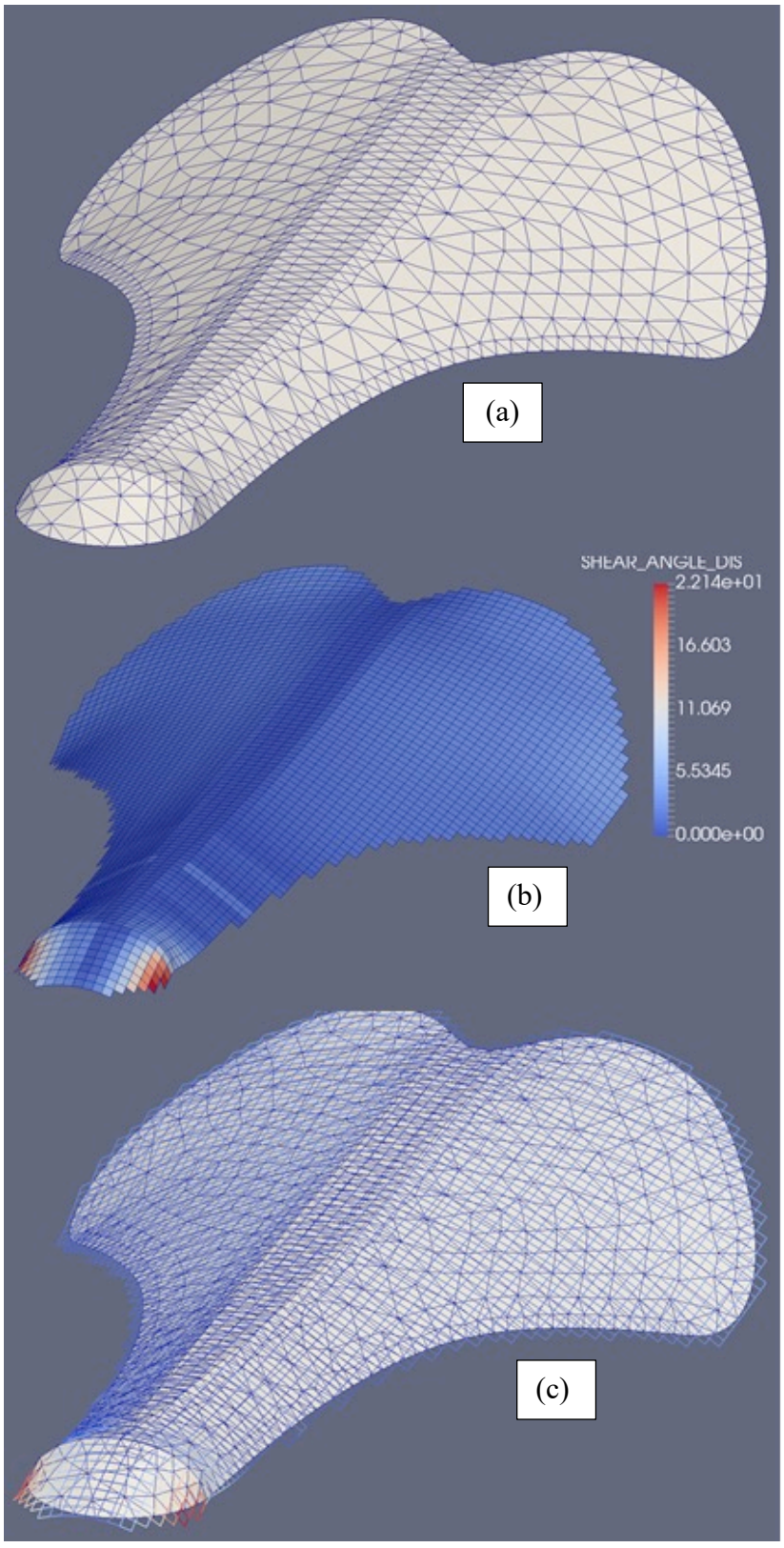

Figure 7- (a) A triangulated bicycle saddle (b) Shear angle distribution of the draped composite (c) The saddle and draped composite together

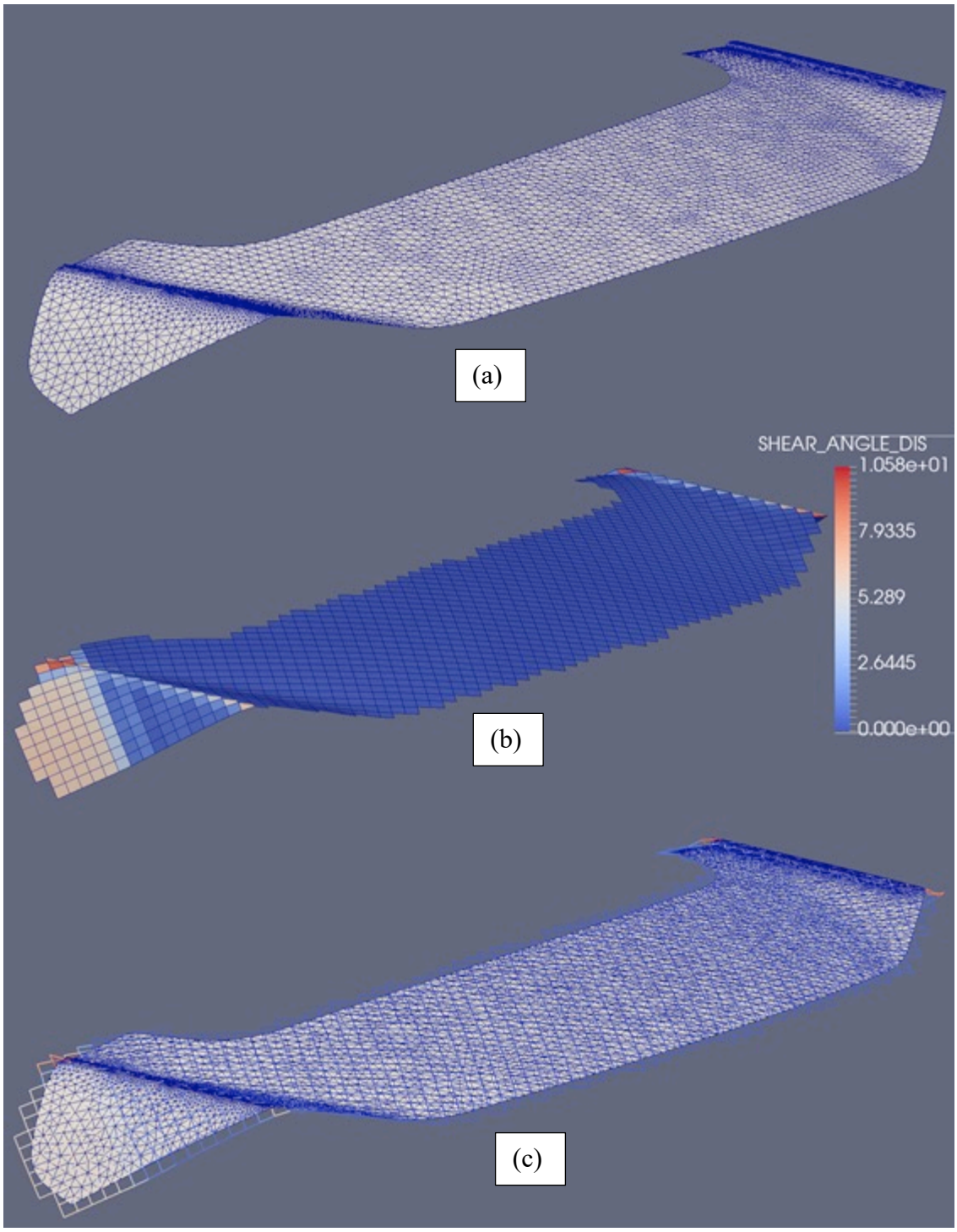

Figure 8- (a) A triangulated car spoiler (b) Shear angle distribution of the draped composite (c) The spoiler and draped composite together

3. FINDING FABRIC FLAT CONTOUR

A byproduct of this draping algorithm is the flat contour of the composite fabric. As mentioned in the introduction, the fabric in this methodology is considered as a group of square (or rectangular) cells. Thus, once the draping of the fabric is done, it can be easily mapped to a 2D plane (e.g. XY plane) to obtain the flattened surface. The boundary of this flat specifies the cut line of this component from the composite fabric sheet.

To find the flat contour, after the draping phase, for all the nodes on the surface boundary, the closest node of the draped fabric is found (e.g. Figure 9). Suppose i and j are the warp-weft indices of this fabric node. In this context, the indices of P_0, the initial seed point, is $(0,0)$ and it is mapped to $(0,0)$ location in the XY plane. Also, from this boundary node B, to vectors parallel to the local warp and weft directions, which form a non-orthogonal basis, could be drawn. Let l_1 and l_2 be the lengths of these vectors, respectively. Then, the location of boundary node B on the XY plane is

$$x = L_{warp} \times i \pm |\vec{l}_1| \qquad y = L_{weft} \times j \pm |\vec{l}_2| \tag{3}$$

Figure 10 and 11 depict the flat contour of some draped composite fabrics.

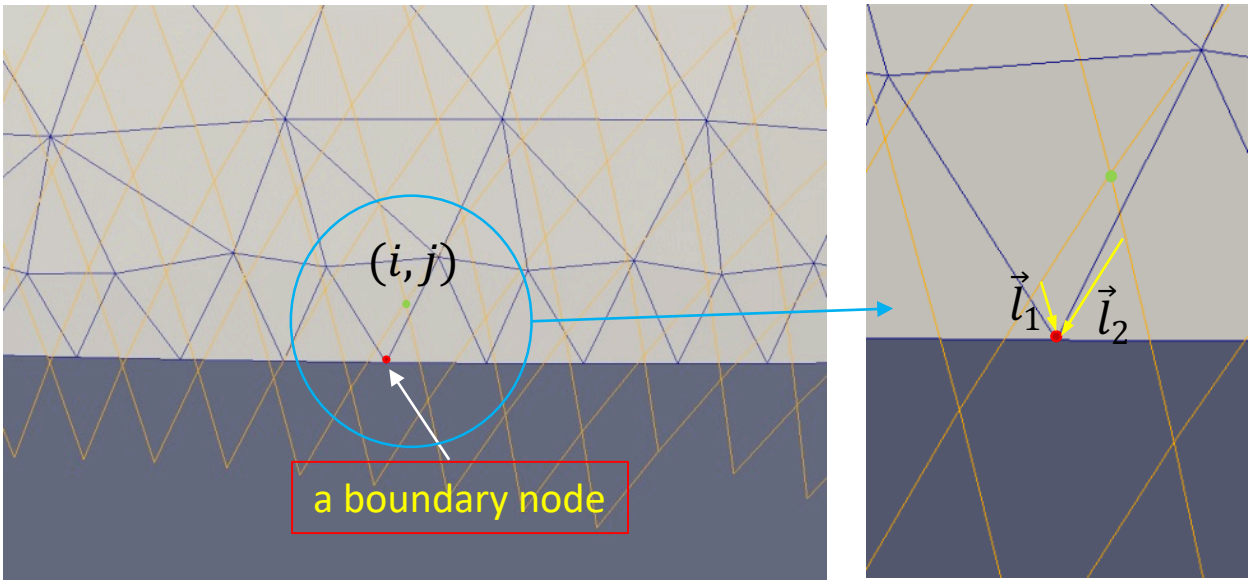

Figure 9- Surface flattening strategy

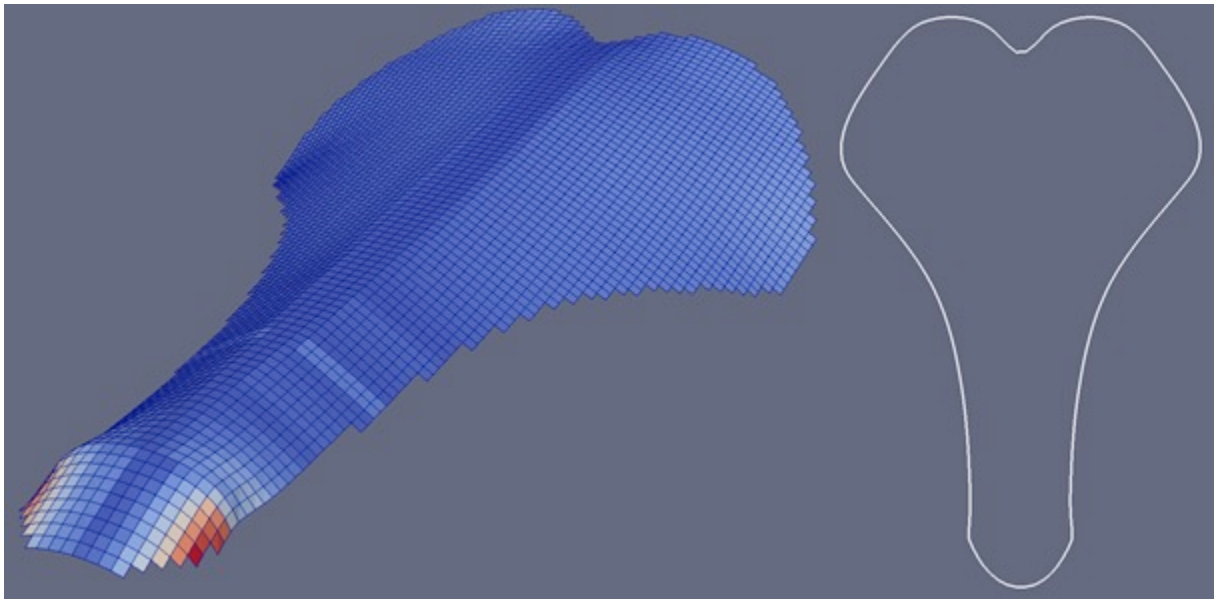

Figure 10- Left: Bicycle saddle draping, Right: Flat contour

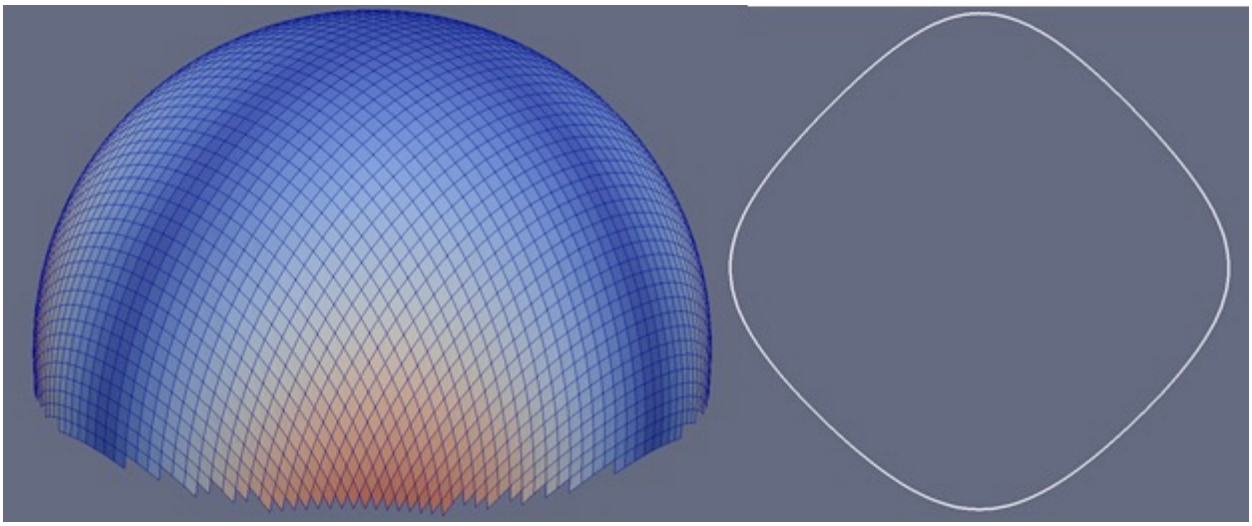

Figure 11- Hemisphere draping, Right: Flat contour

4. APPLYING THESE RESULTS TO THE FORMING PROCESS

Composite forming is a direct extension of the draping process. An FEA method is necessary to simulate this manufacturing process, but it can be seeded with the results from the draping algorithm. By using the presented method, we can reduce the amount of time an FEA calculation takes while maintaining enough accuracy for analyzing the wrinkles and deformations. Figure 12 shows an automotive B-Pillar that was used to test this extension of the draping process. Forming composite components allows for a fast production cycle time, which creates more interest in the automotive industry to manufacture composite parts. The FEA method used simulates a single layer solution with varying material characteristics. A uniform force is distributed across the surface as the mold and die are pressed together. The results are displayed for 3 different materials in Figure 13. This can be extended even further for a stack of material or lamina if a multilayered physical model is applied.

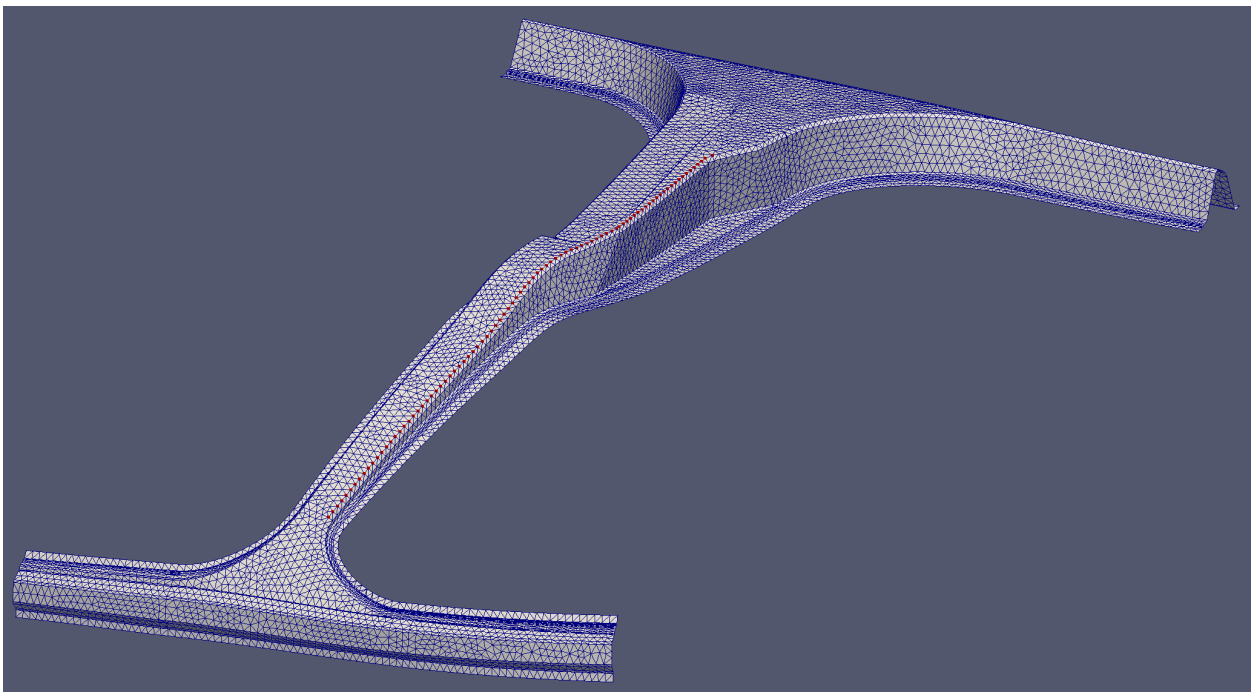

Figure 12- Automotive B-Pillar Example

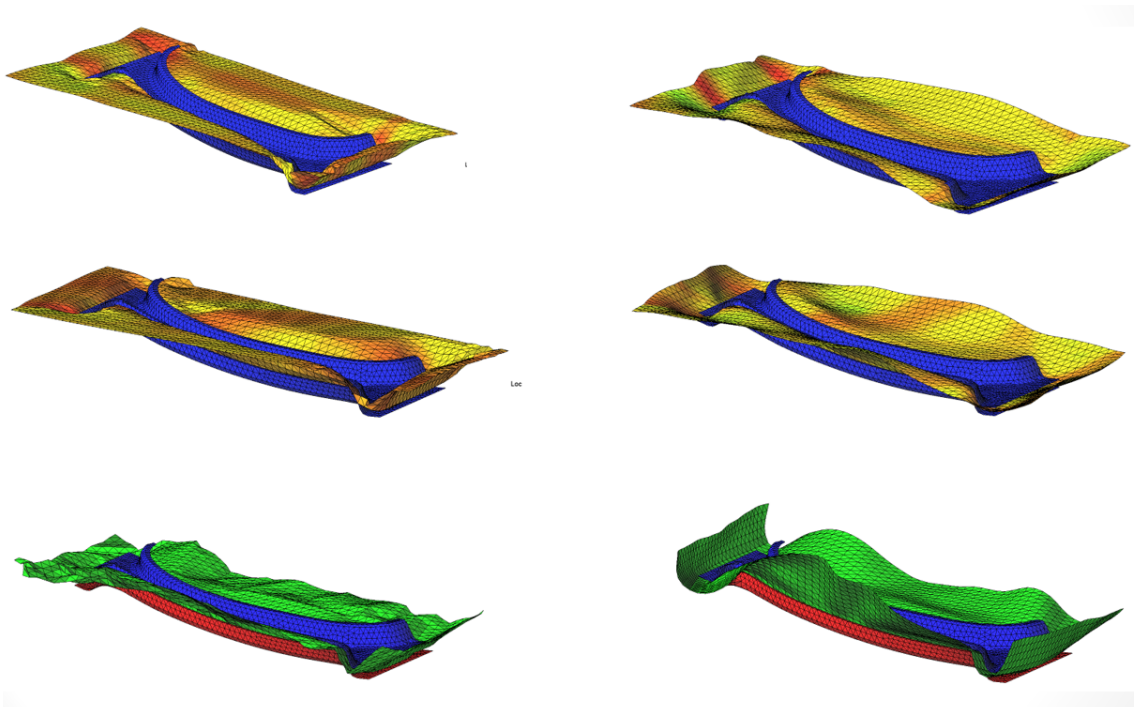

Figure 13- Initial results for Single Layer Forming of different material properties

5. CONCLUSIONS

As we've seen, a hybrid approach used to solve for material draping over a surface can provide multiple benefits. The speed of the calculation provides users the ability to analyze multiple material draping scenarios to quickly iterate on the design for manufacturing process. The hybrid approach also provides results that are accurate enough to make these considerations at the design stage. The flat patterns generated from the draping simulation can be then used to influence an FEA-based forming simulation to again speed up the process and provide more manufacturing information at the design stage. By providing this up front, manufacturers can decrease the amount of manufacturing iterations and design changes that occur after the design process. Manufacturing parts with the forming process lends itself to higher amounts of automation and decreased part cycle times, allowing industries, like the automotive industry, to start taking advantage of composite materials in traditional products. By combining this automation on the shop floor with quick software simulation, manufacturers can now start to produce composite components and leverage design changes in new models year over year.

REFERENCES

[1] P. Boisse, Y. Aimène, A. Dogui, S. Dridi, S. Gatouillat, N. Hamila, M. A. Khan, T. Mabrouki, F. Morestin, and E. Vidal-Sallé, "Hypoelastic, hyperelastic, discrete and semi-discrete approaches for textile composite reinforcement forming", International journal of material forming, vol. 3 (2), pp. 1229–1240, 2010.

[2] P. Boisse, N. Hamila, F. Helenon, B. Hagege, and J. Cao, "Different approaches for woven composite reinforcement forming simulation", International journal of material forming, vol. 1(1), pp. 21–29, 2008.

[3] N. Hamila and P. Boisse, "Simulations of textile composite reinforcement draping using a new semi-discrete three node finite element", Composites Part B: Engineering, vol. 39(6), pp. 999–1010, 2008.

[4] X. Q. Peng and J. Cao, "A continuum mechanics-based non-orthogonal constitutive model for woven composite fabrics", Composites part A: Applied Science and manufacturing, vol. 36(6), pp. 859–874, 2005.

[5] Y. Aimene, E. Vidal-Salle, B. Hagege, F. Sidoroff, and P. Boisse, "A Hyperelastic Approach for Composite Reinforcement Large Deformation Analysis", Journal of Composite materials, vol. 44(1), pp. 5–26, 2010.

[6] G. Kumar, P. Srinivasan, and V. Holla, "Geodesic curve computations on surfaces", Computer Aided Geometric Design, vol. 20(2), pp. 119–133, 2003.